
This is an electronic reprint of the original article.

This reprint may differ from the original in pagination and typographic detail.

Author(s): Kemppinen, A. & Lotkhov, S. V. & Saira, O.-P. & Zorin, A. B. & Pekola, Jukka & Manninen, A. J.

Title: Long hold times in a two-junction electron trap

Year: 2011

Version: Final published version

Please cite the original version:

Kemppinen, A. & Lotkhov, S. V. & Saira, O.-P. & Zorin, A. B. & Pekola, Jukka & Manninen, A. J. 2011. Long hold times in a two-junction electron trap. Applied Physics Letters. Volume 99, Issue 14. P. 142106/1-3. ISSN 0003-6951 (printed). DOI: 10.1063/1.3647557.

Rights: © 2011 American Institute of Physics. This article may be downloaded for personal use only. Any other use requires prior permission of the author and the American Institute of Physics. The following article appeared in Applied Physics Letters and may be found at <http://scitation.aip.org/content/aip/journal/apl/99/14/10.1063/1.3647557>

Long hold times in a two-junction electron trap

A. Kemppinen, S. V. Lotkhov, O.-P. Saira, A. B. Zorin, J. P. Pekola, and A. J. Manninen

Citation: [Applied Physics Letters](#) **99**, 142106 (2011); doi: 10.1063/1.3647557

View online: <http://dx.doi.org/10.1063/1.3647557>

View Table of Contents: <http://scitation.aip.org/content/aip/journal/apl/99/14?ver=pdfcov>

Published by the [AIP Publishing](#)

Articles you may be interested in

[A hybrid superconductor-normal metal electron trap as a photon detector](#)

Appl. Phys. Lett. **100**, 242601 (2012); 10.1063/1.4729417

[Origin of the spin-triplet Andreev reflection at ferromagnet/ s -wave superconductor interface](#)

J. Appl. Phys. **103**, 023921 (2008); 10.1063/1.2837059

[Influence of electron–electron interactions on supercurrent in SNS structures](#)

Low Temp. Phys. **29**, 546 (2003); 10.1063/1.1596575

[Influence of dissipation on a low-voltage dc current in a long SNS junction](#)

Low Temp. Phys. **28**, 547 (2002); 10.1063/1.1496665

[Wave functions of Andreev bound states in superconductor/normal-metal/superconductor junctions](#)

J. Appl. Phys. **91**, 7119 (2002); 10.1063/1.1448784

CREATE

your best design

TE11 cutoff frequency (fc): 4.868 Hz

Frequency: Hz

Wavelength (λ): 0.5205 m

Flare angle: °

Corrugation thickness: m


Corrugation length: m

Horn thickness: m

Horn length: m

Waveguide length: m

Matching corrugation length: m



WITH SIMULATION APPS »

COMSOL

Input waveguide cross pol. ratio: 17.657 %

Output aperture cross pol. ratio: 3.025 %

☒ Target criterion: passed

Long hold times in a two-junction electron trap

A. Kemppinen,^{1,a)} S. V. Lotkhov,² O.-P. Saira,³ A. B. Zorin,² J. P. Pekola,³
and A. J. Manninen¹

¹Centre for Metrology and Accreditation (MIKES), P.O. Box 9, 02151 Espoo, Finland

²Physikalisch-Technische Bundesanstalt, Bundesallee 100, 38116 Braunschweig, Germany

³Low Temperature Laboratory, Aalto University, P.O. Box 13500, 00076 Aalto, Finland

(Received 8 August 2011; accepted 16 September 2011; published online 5 October 2011)

The hold time τ of a single-electron trap is shown to increase significantly due to suppression of photon assisted tunneling events. Using two rf-tight radiation shields instead of a single one, we demonstrate increase of τ by a factor exceeding 10^3 , up to about 10 h, for a trap with only two superconductor (S)—normal-metal (N) tunnel junctions and an on-chip resistor $R \sim 100$ k Ω (R-SNS structure). In the normal state, the improved shielding made it possible to observe $\tau \sim 100$ s, which is in reasonable agreement with the quantum-leakage-limited level expected for the two-electron cotunneling process. © 2011 American Institute of Physics. [doi:10.1063/1.3647557]

Creating a quantum current standard based on frequency-driven single-electron transport has been one of the major goals of metrology for about 25 years.¹ In the 1990's, the efforts were focused mainly on metallic tunnel junction devices. Relative uncertainty of about 10^{-8} was reached by the seven-junction electron pump for small currents at the level of a few pA.² Recent advances^{3–5} have raised the hope to increase the current by factor 10–100 towards a more practical level, renewing the interest to the accuracy issues.

Photon (aka *environmentally*) assisted tunneling (PAT)^{6,7} has been found to limit the transport accuracy at the level far above theoretical predictions.^{8,9} Recently, it was shown that PAT rate Γ in the superconductor (S) – normal metal (N) hybrid turnstile⁵ can be reduced down to time-resolved single events by using on-chip noise filtering elements: a high-ohmic resistor (R-SNS turnstile^{10,11}) or a capacitively coupled ground plane.^{7,12,13} The electron trapping properties of the pumps are important for electron-counting capacitance standards¹⁴ and also a way to study the leakage mechanisms. In the preceding experiment with the R-SNS turnstile-based electron trapping circuit, Ref. 11, a reasonably low value of $\Gamma = \tau^{-1} \sim (20 \text{ s})^{-1}$ was achieved in a strong Coulomb blockade. Here, τ is the average hold time of an electron in the trap.

In this letter, we report on the very same R-SNS trap samples tested in a cryogenic setup with a different type of noise filtering: double rf shielding of the sample stage. We demonstrate more than 1000-fold improvement of τ up to about 10 h. This result is comparable with the hold times previously reported for arrays with 7 or more tunnel junctions^{15,16} or with 4 junctions and a high-ohmic resistor connected in series.¹⁷ With the superconductivity suppressed by a magnetic field, tunneling rates down to the level expected for *two-electron cotunneling*^{18–20} were achieved.

Two nominally similar samples, S_A and S_B , were measured in two cryostats, C_A and C_B , respectively. Both sample stages were equipped with two nested rf radiation shields, see Fig. 1(a). In setup C_A , the signal lines were filtered by

the combination of ThermocoaxTM and powder filters and in C_B only by Thermocoax. One of the connectors in C_B was not perfectly rf tight, and unless otherwise stated, the reported results are from S_A/C_A .²¹ During the preparation of this report, we have applied similar nested rf shielding in studies of sub-gap behaviour of SNS transistors,¹³ and we also became aware of the work of Barends *et al.*²² in which similar techniques were used to lower loss and decoherence in superconducting quantum circuits.

The equivalent circuit of the trapping device is shown in Fig. 1(a). The left junction of an Al–AuPd–Al SNS turnstile is connected to an on-chip Cr resistor with $R \sim 100$ k Ω , and the right junction is terminated by a trapping island whose charge state n_2 is monitored by a capacitively coupled SNS single-electron transistor (SET) electrometer operating in the voltage-bias regime. For the details of sample fabrication, see Ref. 11. At low temperatures, $T < 100$ mK, tunneling in the zero-biased trap is blocked by the energy barrier formed by the quasiparticle excitation energy $\Delta_{Al} = 260$ μ eV $= k_B \times 3.0$ K and charging energies $E_{C1} \approx k_B \times 7.6$ K $> E_{C2} \approx k_B \times 3.3$ K of an electron located in the middle and in the trapping island, respectively. The corresponding stability diagram is shown in Fig. 1(b) with the hold times τ calculated using the orthodox theory of single-electron tunneling¹ for four charge states of the trap in thermal equilibrium.

Electrons can be loaded or unloaded from the trap by ramping the bias voltage V_b and, thus, lowering the energy barrier for one of the two tunneling directions. Due to the energy barrier, the bias voltage dependence of the trapped charge n_2 monitored by electrometer current I_{el} appears hysteretic, see Fig. 1(c). The maximum of the barrier height and, thus, the width of the hysteresis loop can be controlled by the gate voltage V_g which is coupled to the middle island by the gate capacitance C_g . Figure 1(c) shows several ramps of V_b encircling the widest loop which corresponds to an integer value of $n_g \equiv C_g V_g / e$, see Fig. 1(b). Due to finite T and external excitations particularly addressed in this work, the observed switchings between charge states include a random component, leading to an uncertainty of the loop width and to the two-level fluctuator behavior depicted in Fig. 1(d).

^{a)}Electronic mail: antti.kemppinen@mikes.fi.

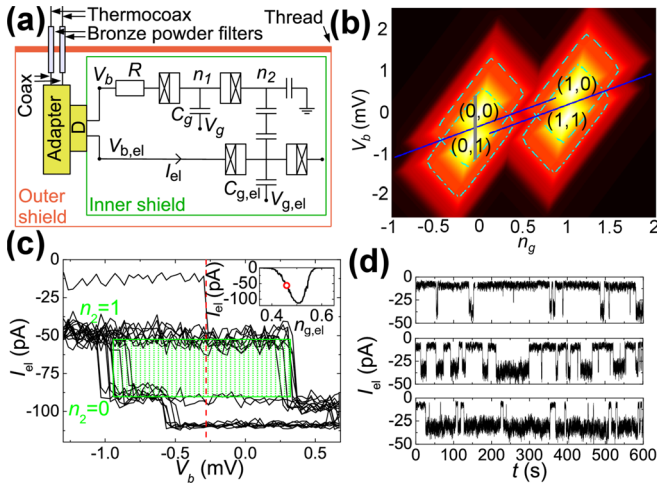


FIG. 1. (Color online) (a) Circuit diagram of the trapping device and schematic of the sample stage of cryostat C_A . The outer shield is a $\phi 14$ cm cylinder mounted to the flange by a thread. The powder filters, screwed to the flange, are used as rf-tight feedthroughs. The signal lines (two of which are shown) are shielded all the way from the filters to the box-shaped inner shield, which is mounted with a D connector and closed with screws. The number of electrons on the normal-metal (AuPd) middle island, n_1 , and on the superconducting (Al) trap island, n_2 , can be controlled by the voltages V_b and V_g . (b) Simulated contour plot of τ at 120 mK for four charge configurations (n_1, n_2) as a function of (n_g, V_b), $n_g \equiv C_g V_g/e$. Bright and dark areas denote long and short values of τ , respectively. In the bistable areas, the largest values of τ are plotted. Inclined rectangles around each stable charge state correspond to $\tau = 1$ s escape thresholds. Two inclined solid lines show the middle points of the hysteresis loops for the states (0, 0)–(0, 1) and (1, 0)–(1, 1). (c) Repeated V_b sweeps around the widest hysteresis loop of about 1.4 mV, emphasized by the rectangle corresponding to the wide grey vertical line in (b). The dashed line in the middle denotes the symmetric case, with equal values of τ for both charge states involved. Inset: Electrometer signal I_{el} as a function of gate voltage $V_{g,el} = C_{g,el} V_{g,el}/e$. The circle denotes a typical operating point. (d) Random switchings of the trap between two charge states. The trap is tuned to exhibit experimentally convenient hold times by setting the width of the hysteresis loop to about 100 μ V. The central panel shows the symmetric case with V_b set in the middle of a hysteresis loop ($\Delta V_b = 0$), while the upper and lower traces are for $\Delta V_b = \mp 7 \mu$ V which favor one of the states.

To support the conclusions of the long hold times shown below, we studied τ as a function of the energy barrier (electrostatic energy change) of tunneling, ΔE , which can be controlled by voltages V_b and V_g . Two-state switching traces were analyzed statistically for different values of ΔE . Figure 2(a) shows typical dependencies of τ on the deviation of bias voltage from the middle of the hysteresis loop (ΔV_b) for three different values of the electrometer current I_{el} . When $\Delta V_b = 0$, ΔE is the same for the two values of n_2 . A shift in ΔV_b shifts proportionally both values of ΔE but in opposite directions. The observed linear dependency of $\log(\tau)$ on ΔE is typical for thermal activation (TA, cf. e.g., Ref. 15): $\tau \propto \exp(-\Delta E/(k_B T^*))$, where the effective temperature T^* characterizes the spectrum of fluctuations driving the state switchings.

To study the crossover from TA to PAT, we present a plot in Fig. 2(b) summarizing the hold time data τ versus ΔE for different electrometer currents I_{el} . For this approximative plot, we used the following conventions: (i) The origin of the ΔE axis was chosen arbitrarily as the point where $\tau \approx 0.1$ s. (ii) The proportionality between ΔE and ΔV_b is based on the fitted stability diagram. (iii) For the curves with the smallest

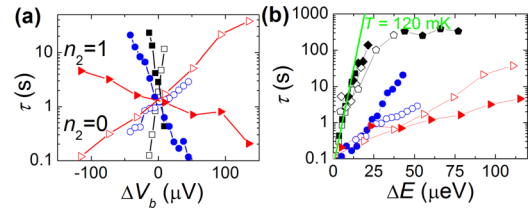


FIG. 2. (Color online) (a) Average hold time τ of two charge states as a function of bias voltage deviation ΔV_b from the middle of the hysteresis loop measured at three different levels of the electrometer current: $I_{el} < 100$ pA (squares), $I_{el} \approx 300$ pA (circles), and $I_{el} \approx 750$ pA (triangles). Open and filled symbols of the same type correspond to the two alternating charge states within the trace: $n_2 = 0$ and $n_2 = 1$, respectively [see Figs. 1(c) and 1(d)]. For each I_{el} , V_g was adjusted such that $\tau \approx 1$ s at $\Delta V_b = 0$. (b) Summarizing plot: hold time τ vs. energy barrier ΔE . The line shows the slope corresponding to thermal activation at $T^* = 120$ mK. Symbols are as in (a). Diamonds and pentagons were measured at $I_{el} < 100$ pA with a wider hysteresis loop than squares.

I_{el} (yielding the longest hold times), we combined the piecewise-continuous data sets measured at different V_g and arranged them along the ΔE axis in Fig. 2(b) to ensure their smooth alignment. This was done because collecting the statistics for a short-living state would take impractically long if following a large hysteresis loop: switching back from the long-living counter state would take hours.

Although Fig. 2(b) is approximative, it allows us to make several conclusions. For small $I_{el} < 100$ pA, a well distinguished slope of $\log(\tau)$ vs. ΔE corresponding to $T^* \approx 120$ mK is observed when $\tau \leq 100$ s. The typical electron temperature in cryostat C_A is lower, about 50 mK, so even in this case, there are still contributing mechanisms beyond the pure TA process. For higher barriers and longer hold times, the slope is much lower, corresponding to $T^* \sim 1$ K. We presume that the shallow slopes are due to PAT at frequency $f \sim \Delta E/h$, activated either by residual photons leaking inside the shields or by the back-action of the electrometer. It generates random telegraph noise (RTN) whose power spectrum has a relatively slow decay $S(\omega) \propto 1/f^2$ in the relevant frequency scale $f \gg I_{el}/e$ (for more details, see Ref. 13). The electrometer back-action is obviously dominant at the larger values of I_{el} , but it cannot be ruled out even in the case of low I_{el} and high ΔE .

Our main result, very long hold time, was achieved with the widest hysteresis loop, i.e., the highest energy barrier $\Delta E \sim (\Delta A_l + E_{C1}) \sim k_B \times 10$ K and $I_{el} < 100$ pA. In this case, the hold time was too long to obtain statistically valid data, but the example of Fig. 3(a) shows a 36-h trace during which the state changed only once. This should be compared with the maximum $\tau \sim 20$ s for the same sample reported in Ref. 11. At higher I_{el} , see Fig. 3(b), the electrometer back-action imposes a significant limitation for the maximum τ . We also did some measurements with sample S_B in cryostat C_B . The maximum hold times were of the order of 1 h. The difference was most likely due to a lower quality of the radiation shielding.

The trapping times for sample S_B were studied also in the normal state in a magnetic field in cryostat C_B . A data trace near the maximum of the hysteresis is shown in Fig. 3(c). Contrary to the NS hybrid state, where two-electron cotunneling is suppressed by the superconducting energy

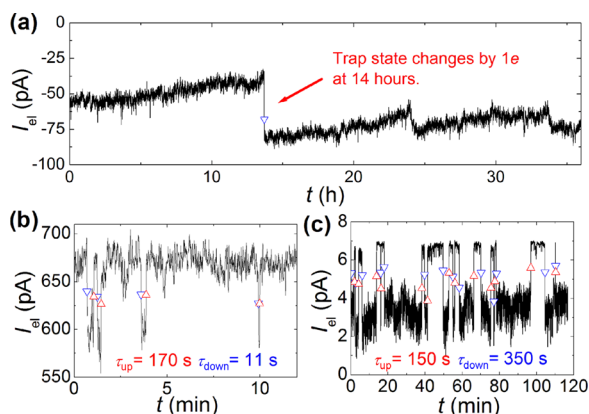


FIG. 3. (Color online) (a) Electrometer data trace at the maximum hysteresis shown in Fig. 1(c) and at low I_{el} . The trap state changed only once at $t \approx 14$ h. Slow drifts in I_{el} are caused by background charge fluctuations of the electrometer. (b) Switching trace at the maximum hysteresis with higher $I_{el} > 500$ pA. (c) Normal state switching trace for sample S_B .

gap,^{5,9} this leakage mechanism can dominate in the normal state if PAT is suppressed strongly enough. Experimental results are in reasonable agreement with the expected cotunneling rate corresponding to $\tau \sim 100$ s, which we estimated following the approximations of Ref. 19 for the case of dissipative environment. For a similar structure without the resistor, the expected value for τ is of the order of 0.1 ms. We note that the cotunneling rates are very sensitive to the parameters of the trap, which we have estimated rather indirectly. Hence, an exact quantitative comparison between theory and experiments would require that the parameters were determined by measuring the IV curve of the trap, for instance, with the help of a cryogenic switch.² Nevertheless, our observations indicate that a high degree of shielding of the sample space makes it possible to reach and study a quantum-leakage-limited behaviour of SET circuits in the normal state.

To conclude, a 1000-fold extension of the hold times was achieved for a two-junction R-SNS electron trap by enclosing it into a specially designed low-noise environment. In the normal state, a switching rate near the quantum leakage floor set by the resistively suppressed two-electron cotunneling was achieved. The hold times of the trap have been measured for the same device over a wide dynamic range from 0.1 s to about 10^4 s, showing high sensitivity to environmental fluctuations, including the back-action from the SET electrometer. Device application for sensitive on-chip noise spectrometry seems feasible.

We acknowledge H. Koivula for advice in rf issues, O. Hahtela and E. Mykkänen for contributions in building the measurement system, and T. Aref for assistance in measurements. The work was partially supported by Technology Industries of Finland Centennial Foundation and by the Finnish Academy of Science and Letters, Väisälä Foundation. The research conducted within the EURAMET joint research project REUNIAM and EU project SCOPE has received funding from the European Community's Seventh Framework Programme under Grant Agreements Nos. 217257 and 218783.

- ¹D. V. Averin and K. K. Likharev, *J. Low Temp. Phys.* **62**, 345 (1986).
- ²M. W. Keller, J. M. Martinis, N. M. Zimmerman, and A. H. Steinbach, *Appl. Phys. Lett.* **69**, 1804 (1996).
- ³J. E. Mooij and Y. V. Nazarov, *Nat. Phys.* **2**, 169 (2006).
- ⁴M. D. Blumenthal, B. Kaestner, L. Li, S. Giblin, T. J. B. M. Janssen, M. Pepper, D. Anderson, G. Jones, and D. A. Ritchie, *Nat. Phys.* **3**, 343 (2007).
- ⁵J. P. Pekola, J. J. Vartiainen, M. Möttönen, O.-P. Saira, M. Meschke, and D. V. Averin, *Nat. Phys.* **4**, 120 (2008).
- ⁶R. L. Kautz, M. W. Keller, and J. M. Martinis, *Phys. Rev B* **62**, 15888 (2000).
- ⁷J. P. Pekola, V. F. Maisi, S. Kafanov, N. Chekurov, A. Kemppinen, Y. A. Pashkin, O.-P. Saira, M. Möttönen, and J. S. Tsai, *Phys. Rev. Lett.* **105**, 026803 (2010).
- ⁸R. L. Kautz, M. W. Keller, and J. M. Martinis, *Phys. Rev B* **60**, 8199 (1999).
- ⁹D. V. Averin and J. P. Pekola, *Phys. Rev. Lett.* **101**, 066801 (2008).
- ¹⁰S. V. Lotkhov, A. Kemppinen, S. Kafanov, J. P. Pekola, and A. B. Zorin, *Appl. Phys. Lett.* **95**, 112507 (2009).
- ¹¹S. V. Lotkhov, O.-P. Saira, J. P. Pekola, and A. B. Zorin, *New J. Phys.* **13**, 013040 (2011).
- ¹²O.-P. Saira, M. Möttönen, V. F. Maisi, and J. P. Pekola, *Phys. Rev. B* **82**, 155443 (2010).
- ¹³O.-P. Saira, A. Kemppinen, V. F. Maisi, and J. P. Pekola, e-print arXiv:1106.1326 (2011).
- ¹⁴M. W. Keller, A. L. Eichenberger, J. M. Martinis, and N. M. Zimmerman, *Science* **285**, 1706 (1999).
- ¹⁵P. D. Dresselhaus, L. Ji, S. Han, J. E. Lukens, and K. K. Likharev, *Phys. Rev. Lett.* **72**, 3226 (1994).
- ¹⁶V. Krupenin, S. Lotkhov, and D. Presnov, *J. Exp. Theor. Phys.* **84**, 190 (1997).
- ¹⁷S. V. Lotkhov, H. Zangerle, A. B. Zorin, and J. Niemeyer, *Appl. Phys. Lett.* **75**, 2665 (1999).
- ¹⁸D. V. Averin and A. A. Odintsov, *Phys. Lett. A* **140**, 251 (1989); D. V. Averin and Y. V. Nazarov, *Phys. Rev. Lett.* **65**, 2446 (1990).
- ¹⁹A. A. Odintsov, V. Bubanja, and G. Schön, *Phys. Rev. B* **46**, 6875 (1992).
- ²⁰D. S. Golubev and A. D. Zaikin, *Phys. Lett. A* **169**, 475 (1992).
- ²¹Most inside walls of the shields in cryostat C_A were painted by an absorptive material (copper powder-epoxy mixture). However, noise levels obtained in Ref. 13 in an improved version of C_B without absorbers were as low as in C_A .
- ²²R. Barends, J. Wenner, M. Lenander, Y. Chen, R. C. Bialczak, J. Kelly, E. Lucero, P. O'Malley, M. Mariantoni, D. Sank, H. Wang, T. C. White, Y. Yin, J. Zhao, A. N. Cleland, J. M. Martinis, and J. J. A. Baselmans, *Appl. Phys. Lett.* **99**, 113507 (2011).